Electronic Supplementary Information

for

An unexpected in-solution instability of diiodido analogue of *picoplatin* complicates its biological characterization

Pavel Štarha *, Bohuslav Drahoš and Radovan Herchel

Department of Inorganic Chemistry, Faculty of Science, Palacký University in Olomouc, 17. listopadu 1192/12, 771 46 Olomouc, Czech Republic

Corresponding Author:

* E-mail: pavel.starha@upol.cz (P.Š.)

Table of contents

Experimental Section

Materials

The chemicals $K_2[PtCl_4]$, KI, KCl, KOH, diammine-dichloridoplatinum(II) (*cisplatin*), NH_3 (25% water solution), HCl (35% water solution), 2-methylpyridine (α-picoline, pic), $AgNO_3$, solvents diethyl ether, *N*,*N*-dimethylformamide (DMF), dimethyl sulfoxide (DMSO), methanol (MeOH), ethanol (EtOH), acetonitrile (MeCN), deuterated solvents (DMF-d_7, D_2O) and HPLC grade solvents (MeCN, H_2O) were supplied by VWR International or Sigma-Aldrich.

Syntheses

Complex K[PtCl$_3$(NH$_3$)]. Complex $K[PtCl_3(NH_3)]$ was prepared as described previously.[1–3] A yield was 37 %. *Anal*. Calc. for H_3NCl_3KPt: H, 0.9; N, 3.9; found: H, 0.8; N, 4.0 %.

Complex *cis*-[PtI$_2$(NH$_3$)(pic)] (1). Complex **1** was prepared as described previously.[3] Briefly, $K[PtCl_3(NH_3)]$ (50 mg, 0.14 mmol) was dissolved in *ca.* 2 mL of distilled water and a slight excess of KI (72 mg, 0.43 mmol). After 10 min of stirring in the dark at the laboratory temperature, when the yellow mixture changed the colour to dark brown ($K[PtI_3(NH_3)]$ formed), α-picoline (12 mg, 0.13 mmol) was poured in. The brown precipitate of complex *cis*-$[PtI_2(NH_3)(pic)]$ (**1**), which formed within 30 min of stirring at laboratory temperature, was removed by filtration and washed with water. The product (**1**) was dried in desiccator under reduced pressure. A yield was *ca.* 83 %. Complex **1** was negligibly soluble in water or MeOH, but well-soluble in DMF and DMSO. A purity of **1** was confirmed by elemental analysis and ^{1}H NMR.

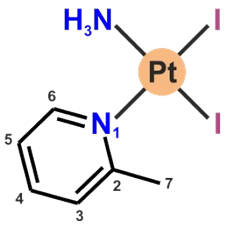

Anal. Calc. for $C_6H_{10}N_2I_2Pt$: C, 12.9; H, 1.8; N, 5.0; found C, 12.8; H, 1.4; N, 5.4 %. ^{1}H NMR (DMF-d_7, 300 K, ppm): 8.98 (d, J = 5.1 Hz, C6–H), 7.92 (td, J = 7.3, 1.5 Hz, C4–H), 7.57 (d, J = 7.3 Hz, C3–H), 7.41 (t, J = 6.6 Hz, C5–H), 4.36 (bs, NH_3), 3.17 (s, C7–H). ^{13}C NMR (DMF-d_7, 300 K, ppm): 162.0 (C2), 153.8 (C6–H), 139.3 (C4–H), 127.7 (C3–H), 123.9 (C5–H), 26.2 (C7–H3). ^{15}N NMR (DMF-d_7, 300 K, ppm): 230.1 (N1), –44.3 (NH_3). ESI+ MS (MeOH): 490.9 (calcd. 490.9; 60%; $\{[PtClI(NH_3)(pic)]+Na\}^+$), 432.0 (calcd. 432.0; 10%; $[PtI(NH_3)(pic)]^+$), 304.1 (calcd. 304.1; 40%; $\{[Pt(NH_3)(pic)]–H\}^+$), 94.2 (calcd. 94.1; 40%; $\{pic+H\}^+$). FTIR (ν_{ATR}, cm^{-1}): 3562w, 3324w, 3246s, 3159s, 2991w,

2723w, 1645w, 1607s, 1567m, 1539w, 1477s, 1453s, 1418m, 1375m, 1361w, 1295vs, 1239m, 1157m, 1111m, 1066w, 1034m, 989w, 792m, 761vs, 716m, 482w, 445w.

Complex *cis*-[$PtCl_2(NH_3)$(pic)] (2; *picoplatin*). Complex **2** was prepared as described previously.[3] Briefly, complex *cis*-[$PtI_2(NH_3)$(pic)] (90 mg, 0.16 mmol) was dissolved in a minimum volume of MeOH and a stoichiometric amount of $AgNO_3$ (55 mg, 0.32 mmol) was added. The mixture was stirred in the dark for 24 h at laboratory temperature and then the formed precipitate of AgI was removed. The obtained filtrate was added with KCl (42 mg, 0.56 mmol), leading to the formation of yellow precipitate of **2** (3 h of stirring, laboratory temperature). The product was removed by filtration, washed with water, EtOH and diethyl ether, and dried in desiccator under reduced pressure. A yield was 40 %.

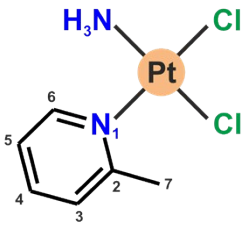

Anal. Calc. for $C_6H_{10}N_2Cl_2Pt$: C, 19.2; H, 2.7; N, 7.5; found: C, 18.9; H, 2.4; N, 7.2 %. ^{1}H NMR (DMF-d_7, 300 K, ppm): 9.02 (d, J = 5.1 Hz, C6–H), 7.86 (m, C4–H), 7.56 (d, J = 8.1 Hz, C3–H), 7.34 (t, J = 6.6 Hz, C5–H), 4.41 (s, NH_3), 3.17 (bs, C7–H). ESI+ MS (MeOH): 399.0 (calcd. 399.0; 40%; $\{[PtCl_2(pic)_2]+Na\}^+$), 304.0 (calcd. 304.1; 20%; $\{[Pt(NH_3)(pic)]-H\}^+$), 94.2 (calcd. 94.1; 5%; $\{pic+H\}^+$). FTIR (ν_{ATR}, cm^{-1}): 3521w, 3478w, 3269s, 3190s, 3067m, 2973m, 2734w, 2648w, 2396w, 2165w, 1630w, 1609s, 1566m, 1478s, 1449s, 1377vs, 1324vs, 1297vs, 1156m, 1112m, 1065m, 1037m, 885w, 824m, 803w, 768s, 717m, 484w, 448w.

Complex *cis*-[$Pt(H_2O)(NH_3)(OH)$(pic)]$^+$. Complex *cis*-[$PtI_2(NH_3)$(pic)] (0.67 mg) was dissolved in the mixture of MeCN or DMF (750 µL) and H_2O (750 µL) and two molar equivalents of $AgNO_3$ (0.41 mg) were added. The mixture was stirred in the dark for 24 h at laboratory temperature and AgI, which formed by this reaction, was removed. The obtained solution of *cis*-[$Pt(H_2O)(NH_3)(OH)$(pic)]$^+$ was used as a control for the HPLC (50% MeCN/50% H_2O mixture) and UV-Vis (50% DMF/50% H_2O mixture) studies.

General methods

Elemental analyses (C, H, N) were carried out by a Flash 2000 CHNS Elemental Analyser (Thermo Scientific). ^{1}H NMR, ^{13}C NMR, ^{1}H–^{1}H gs-COSY, ^{1}H–^{13}C gs-HMQC, ^{1}H–^{13}C gs-HMBC and ^{1}H–^{15}C gs-HMBC spectra (for **1**) and ^{1}H NMR spectra (for **2**) were recorded using a JEOL JNM-ECA 600II spectrometer and the spectra were calibrated against the residual signals of the used solvents.[4] Mass spectrometry was performed on the MeOH

solution using a LCQ Fleet Ion Trap spectrometer (Thermo Scientific; Qual Browser software, version 2.0.7) in the positive electrospray ionization mode (ESI+). FTIR spectra were recorded by a Nexus 670 FT-IR spectrometer (Thermo Nicolet) using an ATR technique (the 400–4000 cm^{-1} region).

^{1}H NMR studies

Complex **1** (0.67 mg) or **2** (0.45 mg) were dissolved in 600 μL of DMF-d_7 or in the mixture of 300 μL of DMF-d_7 and 300 μL of D_2O (2 mM final concentration). ^{1}H NMR spectra were recorded on the fresh solutions and after 6, 24, 48, 72 and 96 h of standing at 37 °C. ^{1}H NMR spectrum of free α-picoline was recorded as well for comparative purposes.

HPLC studies

Reversed-phase high-performance liquid chromatography coupled to the positive electrospray ionization mode mass spectrometry (RP-HPLC/ESI+ MS) was carried out using UHPLC-MS (Dionex/Thermo Fisher Scientific) equipped with an ReproSil-Pur Basic C18 (5 μm pore size, 200 × 4.6 mm). The detection wavelength was 254 nm. Mass spectrometry was performed using a LCQ Fleet Ion Trap spectrometer (Thermo Scientific; Qual Browser software, version 2.0.7) in the positive electrospray ionization mode (ESI+).

Complex *cis*-[$PtI_2(NH_3)$(pic)] (0.67 mg) or complex *cis*-[$PtCl_2(NH_3)$(pic)] (0.45 mg) was dissolved in 1.5 mL of the 50% MeCN/50% H_2O mixture (*v/v*). The mixture of 0.1% ammonium formate in H_2O (A) and MeCN (B) was used as the mobile phase at gradients of 10 % B (t = 0 min), 80 % B (t = 30 min), 80 % B (t = 40 min), 10 % B (t = 41 min) and 10 % B (t = 55 min) over a 55 min period (1 mL min^{-1} flow rate). RP-HPLC/ESI+ MS experiments were performed immediately after the sample preparation and repeated after 24, 48, 72 and 96 h of standing at 37 °C. Analogical experiments were carried out for complex *cis*-$[Pt(H_2O)(NH_3)(OH)(pic)]^+$ and free pic, both dissolved in the 50% MeCN/50% H_2O (*v/v*) mixture of solvents (for comparative purposes).

UV-VIS spectroscopy

The UV-Vis absorption spectroscopy was performed using the spectrometer Lambda 40 (Perkin-Elmer) at the 250–1000 nm region. Complex *cis*-[$PtI_2(NH_3)$(pic)] (2.79 mg)

was dissolved in 2.5 mL of DMF and 2.5 mL of H_2O was added (1 mM final concentration). Spectra were recorded immediately after the sample preparation and after 6, 24, 48, 72 and 96 h of standing at 37 °C. The spectrum of complex *cis*-$[Pt(H_2O)(NH_3)(OH)(pic)]^+$ dissolved in the same solvent (50% DMF/50% H_2O, *v/v*) was recorded for comparative purposes.

DFT calculations

All theoretical calculations were done with ORCA 4.2 software.[5,6] The DFT calculations employed PBE0 hybrid functional[7] together with the atom-pairwise dispersion correction with the Becke-Johnson damping scheme (D3BJ).[8] The ZORA relativistic approximation[9] with SARC-ZORA-TZVPP for Pt,[10] SARC-ZORA-TZVPP for I,[11] ZORA-def2-TZVP for N, O, Cl and ZORA-def2-SVP for C and H atoms.[12] The SARC/J Coulomb fitting basis set was utilized as an auxiliary basis set.[13] Also, chain-of-spheres (RIJCOSX) approximation to exact exchange was utilized.[14,15] Increased integration grids (Grid7 and Gridx7 in ORCA convention) and tight SCF convergence criteria were used in all calculations. Moreover, the increased radial integration accuracy for Pt, I and Cl atoms was also set. Molecular geometries optimizations as well as frequency calculations for all studied complexes were performed without any symmetry restrictions and applying a conductor-like polarizable continuum model (CPCM) with the Gaussian charge scheme set for water.[16,17] The vibrational analyses confirmed proper convergence for complexes at local energy minimum (no imaginary frequencies) and in the case of the transition states geometries only one imaginary frequency was found corresponding to the correct movement of involved atoms. The thermochemistry data were calculated as implemented in ORCA at 298.15 K and Gibbs free energies were corrected by where the factor of 1.89 kcal/mol due to the change in standard state from gas phase to solution phase.[18] We considered separated reactants to define the energy reference state in order to predict the activation barriers.

Results and discussion

NMR spectroscopy

The characteristic pic signal of its methyl group (*i.e.*, C7–H_3) showed at δ = 3.17 ppm and 26.2 ppm in the ^{1}H and ^{13}C NMR spectrum of **1**, respectively (Fig. S1 and S3). The mentioned ^{1}H NMR resonance of **1** formed cross-peaks at C3 (δ = 127.7 ppm) ↔ H7 and C2 (δ = 162.0 ppm) ↔ H7 in the ^{1}H–^{13}C gs-HMBC spectrum, clearly proving the assignment of the adjacent quartery carbon (C2) and the closest C–H group (C3–H), related to the C7–H_3 group of the pic ligand (Fig. S4). Further, the ^{1}H–^{13}C HMBC long-range correlation peaks were detected between the quartery C2 and all the aromatic C–H groups of the pic ligand (C2 ↔ H6 (δ = 8.98 ppm) ↔ H4 (δ = 7.92ppm) ↔ H3 (δ = 7.57 ppm)) except for the C5–H group in the *para* position to C2.

The ^{1}H–^{15}N HMBC spectrum of **1** contained the NH_3 signal and a set of cross-peaks between N1 nitrogen and hydrogens of pic (N1 (230.1) ↔ H6 ↔ H3 ↔ H5 (δ = 7.41 ppm)), again except for the *para*-oriented hydrogen (C4–H in this case).

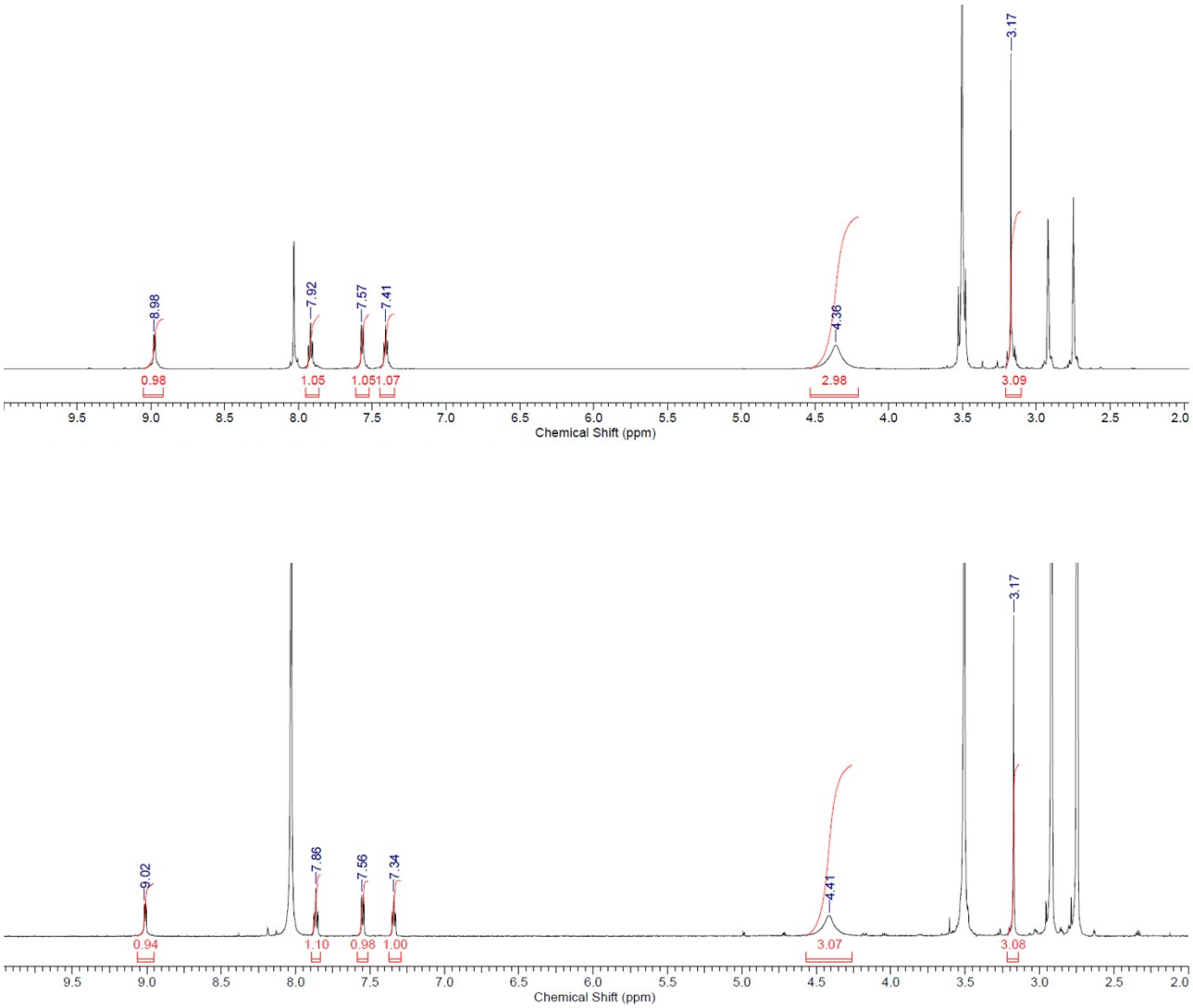

Figure S1. ^{1}H NMR spectra of complexes *cis*-[$PtI_2(NH_3)$(pic)] (**1**; *top*) and *cis*-[$PtCl_2(NH_3)$(pic)] (**2**; *picoplatin*; *bottom*), both dissolved in DMF-d_7.

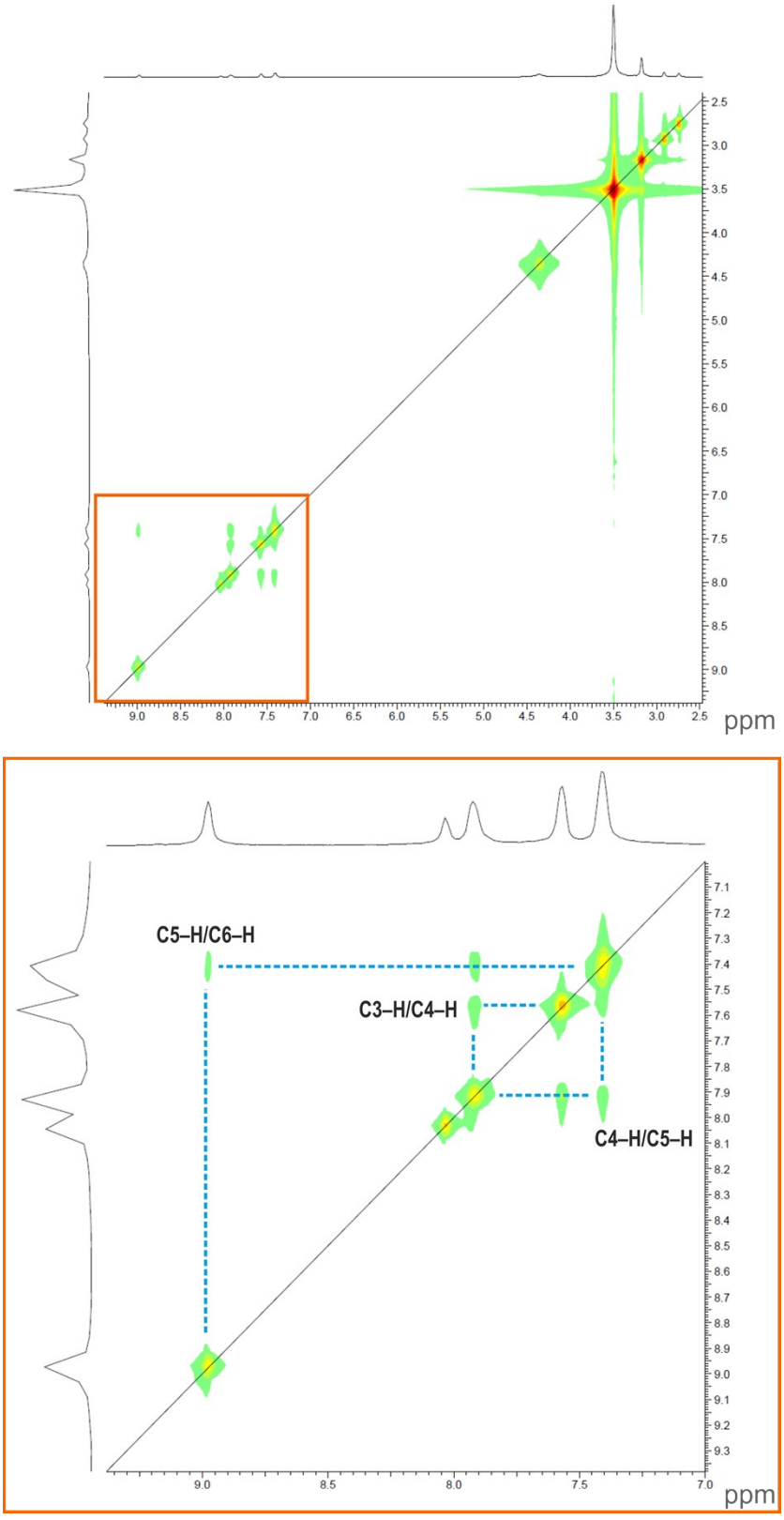

Figure S2. $^{1}H–^{1}H$ gs-COSY spectrum (given at two different resolutions) of complex *cis*-$[PtI_2(NH_3)(pic)]$ (**1**; dissolved in DMF-d_7).

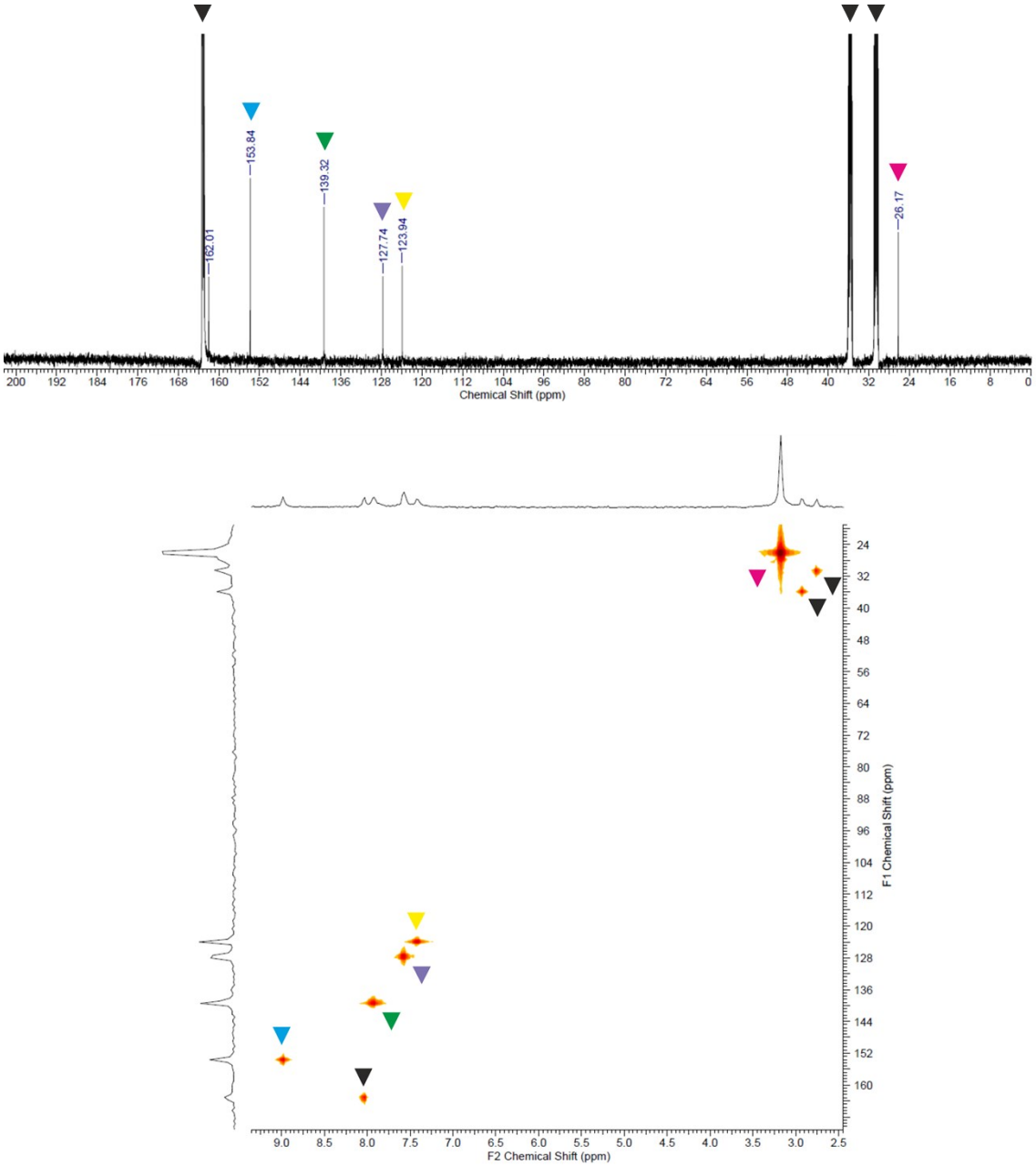

Figure S3. ^{13}C NMR (*top*) and ^{1}H–^{13}C gs-HMQC (*bottom*) spectra of complex *cis*-[$PtI_2(NH_3)$(pic)] (**1**; dissolved in DMF-d_7 (the solvent signals are labelled with black triangles)).

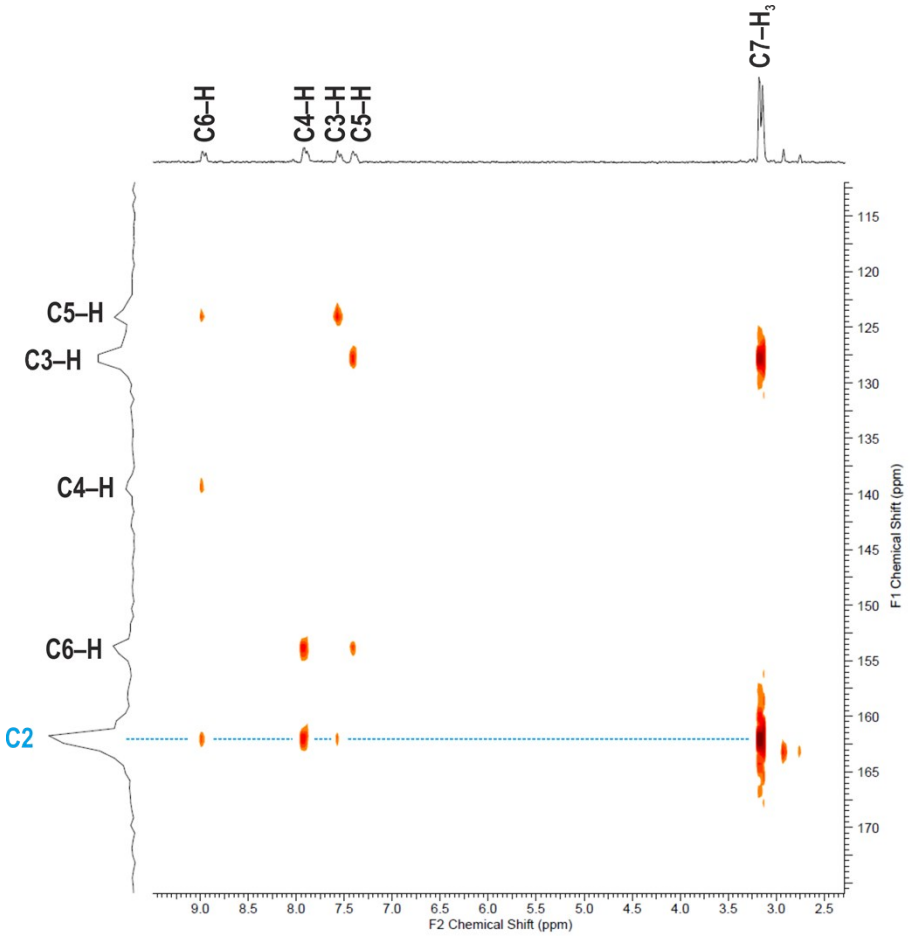

Figure S4. $^{1}H–^{13}C$ gs-HMBC spectrum of complex *cis*-[$PtI_2(NH_3)$(pic)] (**1**; dissolved in DMF-d_7), with the signals of quartery carbon C2 labelled in blue.

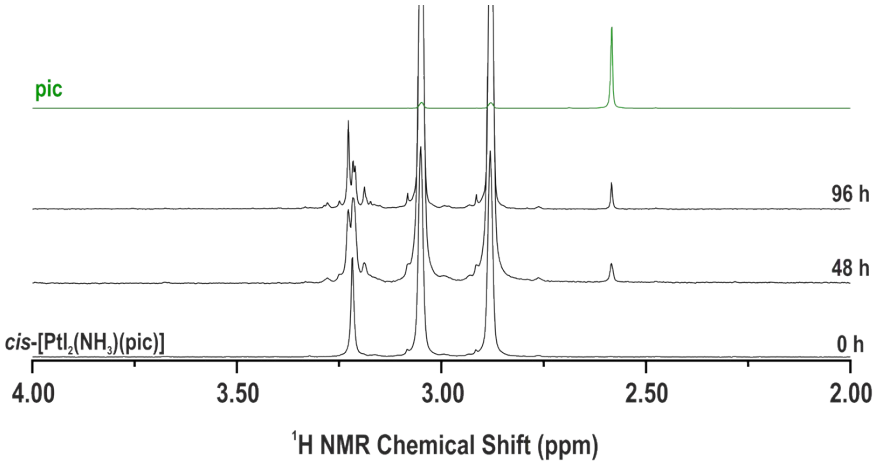

Figure S5. A part of the ^{1}H NMR spectra of complexes *cis*-[$PtI_2(NH_3)$(pic)] (**1**; *black*) at different time points, given together with free 2-methylpyridine (pic; *green*); the samples were prepared in 50% DMF-d_7/50% D_2O and incubated at 37 °C between the individual measurements.

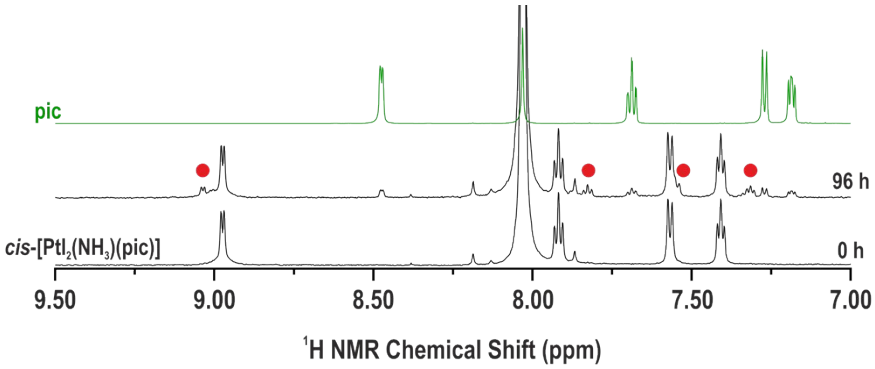

Figure S6. The ^{1}H NMR spectra of complex *cis*-[$PtI_2(NH_3)$(pic)] (**1**; *in black*) at different time points (0 h and 96 h of standing at 37 °C), given together with free 2-methylpyridine (pic; *in green*); both compounds were dissolved in DMF-d_7. The signals assumed for *trans*-[$PtI_2(NH_3)$(pic)] (**1^t**) are labelled with red spheres.

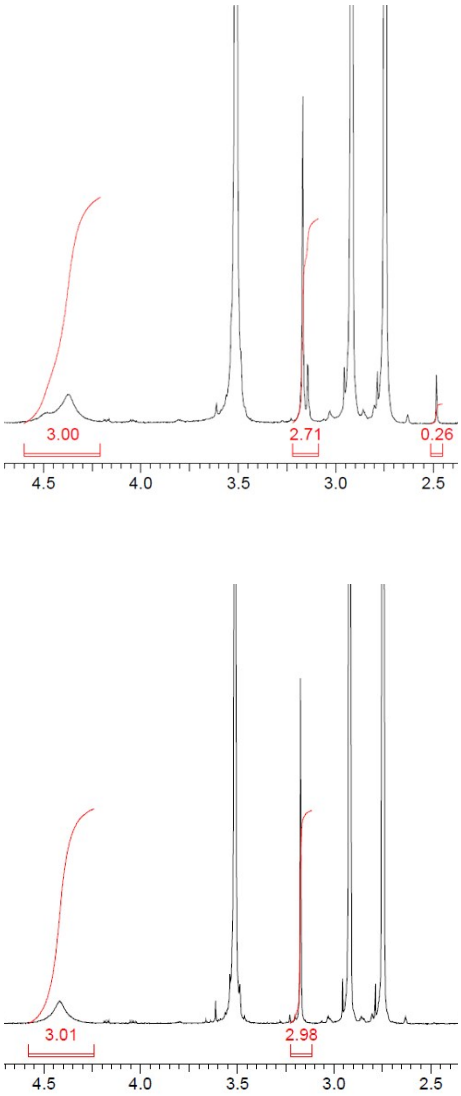

Figure S7. A part of the ^{1}H NMR spectra of complexes *cis*-[$PtI_2(NH_3)$(pic)] (**1**; *top*) and *cis*-[$PtCl_2(NH_3)$(pic)] (**2**; *picoplatin*; *bottom*) after 96 h of standing at 37 °C in DMF-d_7. The total integral intensity of the NH_3 broad signal (4.40 ppm) and the integral intensities of three singlets belonging to the C7–H_3 methyl hydrogens of the initial complex **1** (3.17 ppm), its *trans*-isomer *trans*-[$PtI_2(NH_3)$(pic)] (**1^t**; 3.14 ppm) and the released 2-methylpyridine (pic; 2.48 ppm) (for complex **1**), and the integral intensities of NH_3 (4.42 ppm) and C7–H_3 methyl hydrogens (3.17 ppm) of complex **2** are depicted in the figures as well.

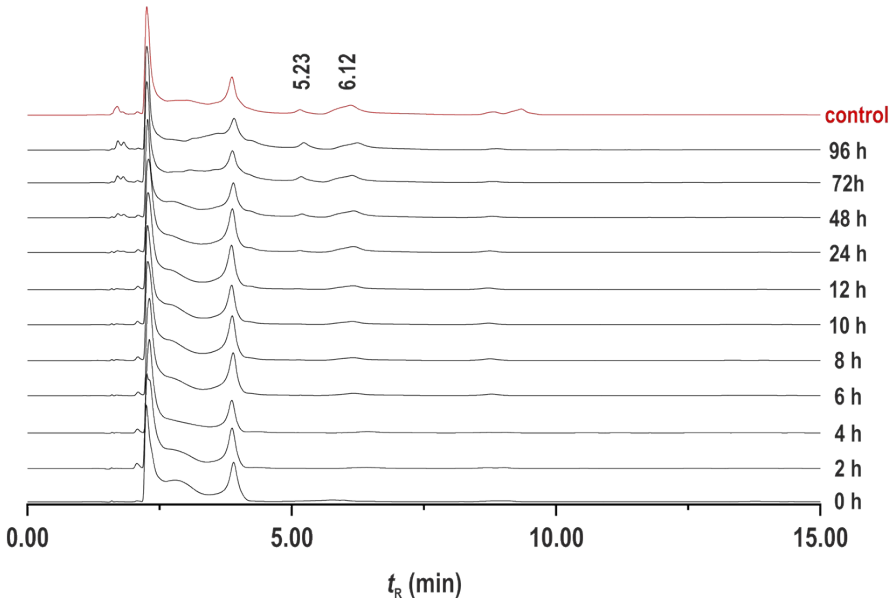

Figure S8. The results of the time-dependent HPLC experiments performed for complexes *cis*-[$PtCl_2(NH_3)$(pic)] (**2**; *picoplatin*; in black), given together with the dechlorinated analogue *cis*-$[Pt(H_2O)(NH_3)(OH)(pic)]^+$ (in red).

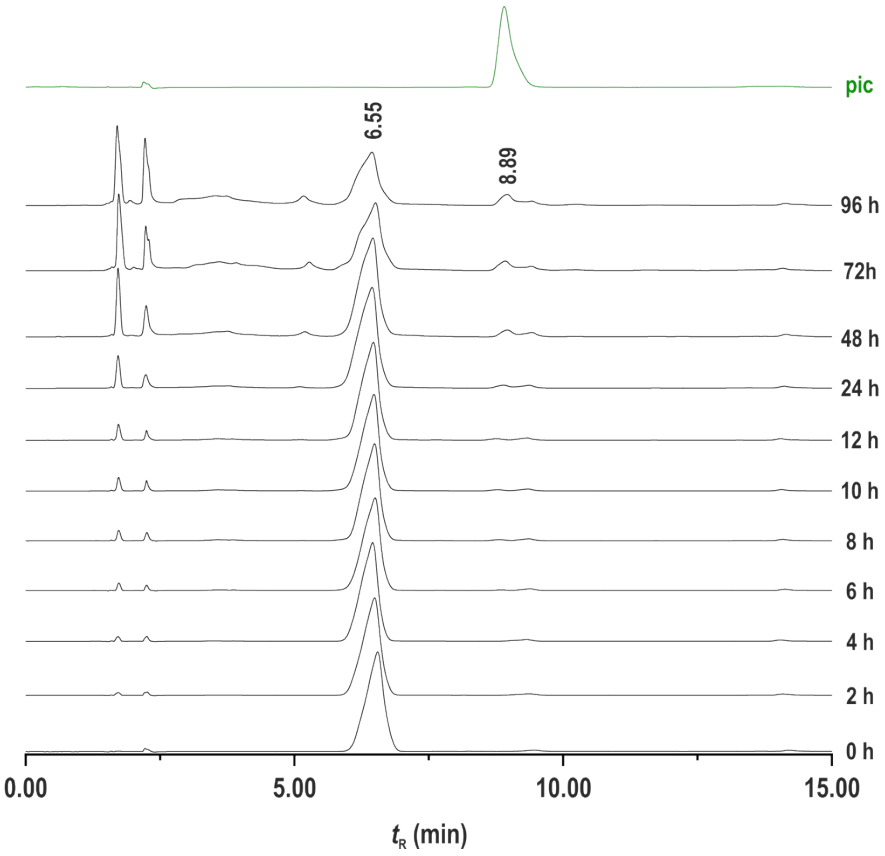

Figure S9. The results of the time-dependent HPLC experiments performed for complexes *cis*-[$PtI_2(NH_3)$(pic)] (**1**; in black), given together with free 2-methylpyridine (pic; in green; t_R = 8.90 min).

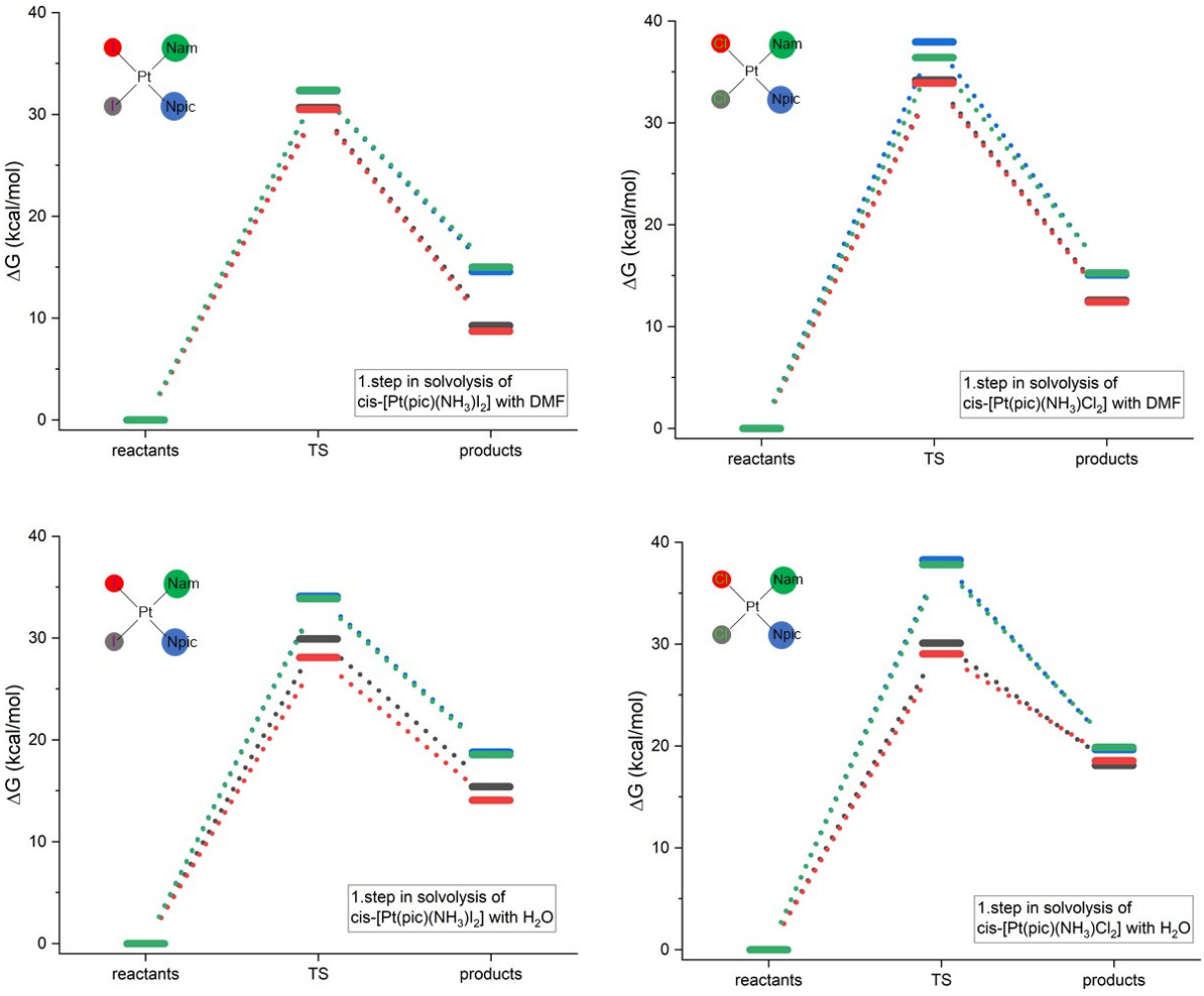

Figure S10. Relative Gibbs free energies of reactants, transition states (TS) and products for the first step of solvolysis of *cis*-[$PtI_2(NH_3)$(pic)] and *cis*-[$PtCl_2(NH_3)$(pic)] (**2**; *picoplatin*) by water and DMF. Colors represents a leaving ligand during the solvolysis.

Table S1. Selected structural parameters for solvolysis of *cis*-[$PtI_2(NH_3)$(pic)] and *cis*-[$PtCl_2(NH_3)$(pic)] by water and DMF calculated by DFT[a]

Solvolysis of *cis*-[$PtX_2(NH_3)$(pic)] by water					
	R1	TS1	P1	TS2	P2
Pt–N_{am}	2.060 (2.038)	2.052 (2.033)	2.059 (2.042)	2.026 (2.016)	2.001
Pt–N_{pic}	2.034 (2.015)	1.993 (1.981)	1.977 (1.976)	1.978 (1.974)	1.977
Pt–X^1 / Pt–X^2	2.612/2.613 (2.304/2.311)	3.052/2.611 (2.776/2.306)	-/2.600 (-/2.293)	-/3.035 (-/2.725)	-/-
Pt–O^1/ Pt–O^2	-/-	2.466/- (2.471/-)	2.071/- (2.068/-)	2.070/2.422 (2.065/2.438)	2.060/2.064
<(A–Pt–B)^{TS}		72.83 (67.67)		73.14 (68.97)	
$\Delta G^{‡}$	-	28.10 (29.04)	-	28.74 (30.13)	-

Solvolysis of *cis*-[$PtX_2(NH_3)$(pic)] by DMF					
	R1	TS1	P1	TS2	P2
Pt–N_{am}	2.060 (2.038)	2.049 (2.029)	2.058 (2.041)	2.039 (2.030)	2.013
Pt–N_{pic}	2.034 (2.015)	1.995 (1.985)	1.987 (1.986)	1.989 (1.985)	1.988
Pt–X^1 / Pt–X^2	2.612/2.613 (2.304/2.311)	3.091/2.616 (2.808/2.312)	-/2.604 (-/2.299)	-/2.998 (-/2.711)	-/-
Pt–O^1/ Pt–O^2	-/-	2.433/- (2.408/-)	2.027/- (2.026/-)	2.023/2.369 (2.024/2.357)	2.022/2.028
<(A–Pt–B)^{TS}		76.48 (75.14)		79.68 (77.13)	
$\Delta G^{‡}$	-	30.49 (33.91)	-	29.91 (33.31)	-

[a] values for *picoplatin* (X = Cl) are in parentheses; bond distances are in Å; X^1 is halogen in the *trans*-position to pic; X^2 is halogen in the *trans*-position to NH_3; A and B are donor atoms of the incoming and the outcoming ligands in the transition state.

Table S2. The selected thermodynamic data of the *cis*-[$PtX_2(NH_3)$(pic)] ↔ *trans*-[$PtX_2(NH_3)$(pic)] isomerization calculated by DFT

X	$\Delta_r H$ (kcal/mol)	$\Delta_r S$ (cal/mol)	$\Delta_r G$ (kcal/mol)
I for *cis/trans*-[$PtI_2(NH_3)$(pic)]	-5.769	1.484	-6.211
Cl for *cis*/*trans*-[$PtCl_2(NH_3)$(pic)]	-2.129	0.414	-2.253

References

1. N. Margiotta, N. Denora, R. Ostuni, V. Laquintana, A. Anderson, S. W. Johnson, G. Trapani and G. Natile, *J. Med. Chem.*, 2010, **53**, 5144.
2. A. R. Battle, R. Choi, D. E. Hibbs and T. W. Hambley, *Inorg. Chem.*, 2006, **45**, 6317.
3. P. Štarha, Z. Trávníček, J. Vančo and Z. Dvořák, *J. Inorg. Biol. Chem.*, 2019, **24**, 257.
4. H. E. Gottlieb, V. Kotlyar and A. Nudelman, *J. Org. Chem.*, 1997, **62**, 7512.
5. F. Neese, F. Wennmohs, U. Becker and C. Riplinger, *J. Chem. Phys.*, 2020, **152**, 224108.
6. F. Neese, *WIREs Comput. Mol. Sci.*, 2018, **8**, e1327.
7. C. Adamo and V. Barone, *J. Chem. Phys.*, 1999, **110**, 6158.
8. (a) L. Goerigk and S. Grimme, *Phys. Chem. Chem. Phys.*, 2011, **13**, 6670; (b) S. Grimme, J. Antony, S. Ehrlich and H. Krieg, *J. Chem. Phys.*, 2010, **132**, 154104.
9. C. van Wüllen, *J. Chem. Phys.*, 1998, **109**, 392.
10. D. A. Pantazis, X.-Y. Chen, C. R. Landis and F. Neese, *J. Chem. Theory Comput.*, 2008, **4**, 908.
11. J. D. Rolfes, F. Neese and D. A. Pantazis, *J. Comput. Chem.*, 2020, **41**, 1842.
12. F. Weigend and R. Ahlrichs, *Phys. Chem. Chem. Phys.*, 2005, **7**, 3297.
13. F. Weigend, *Phys. Chem. Chem. Phys.*, 2006, **8**, 1057.
14. F. Neese, F. Wennmohs, A. Hansen and U. Becker, *Chem. Phys.*, 2009, **356**, 98.
15. R. Izsák and F. Neese, *J. Chem. Phys.*, 2011, **135**, 144105.

16. V. Barone and M. Cossi, *J. Phys. Chem. A*, 1998, **102**, 1995.
17. A. W. Lange and J. M. Herbert, *J. Chem. Phys.*, 2010, **133**, 244111.
18. C. J. Cramer, Essentials of Computational Chemistry: Theories and Models, 2nd Edition, Wiley, 2004.